

Research Article

Full-Scale Experimentation on Building an Integrated Photovoltaic Component for Naturally Ventilated Double-Skin Configuration*

Leon Gaillard,¹ S. Giroux,² H. Pabiou,³ and C. Ménézo¹

¹INSA-Lyon, Chaire INSA-EDF "Habitats et Innovations Energétique," 69100 Villeurbanne, France

²Université Lyon 1, CETHIL, UMR5008, 69621 Villeurbanne, France

³CNRS, CETHIL, UMR5008, 69621 Villeurbanne, France

Address correspondence to C. Ménézo, christophe.menezo@insa-lyon.fr

Received 26 February 2012; Accepted 6 March 2012

Abstract Recent interest in the development of energy-efficient buildings is strongly linked to the global challenge of reducing greenhouse gas emissions in the context of fissile and fossil fuel resource depletion. Photovoltaic (PV) systems offer a promising solution for clean local electricity generation and enhanced cooling and/or heating through natural or forced convection. In this paper we present the "Ressources" project, a study of such components developed at a large scale (for new build and refurbishment). Ressources is part of the French National Research Agency program dedicated to energy and buildings. To date studies have focused on 3 prototype building envelopes comprising naturally ventilated double-skin configurations on real buildings: two for single-family homes (at Moret-sur-Loing—EDF R&D site) and one for an office building (at Toulouse—HBS Technal site). This paper focuses on the latter system and first experimental results obtained in summer 2011.

Keywords BIPV; natural convection; chimney effect

1 Introduction

Most European countries have set the target of reducing greenhouse gas emissions by a factor of 4 by 2050 compared to 1990, and a 20% reduction by 2020 while increasing by 20% the share of renewable energy. The building sector accounts for a large portion of total energy consumption, and hence improvements in this field can contribute significantly to national objectives. Regulations in France will require new buildings from 2020 to be energy-positive (BEPOS). This necessitates improvements to insulation, passive energy storage, and air-tightness, but also a diversification of electrical and thermal energy production, and co-generation

solutions. This implies a redefinition of the envelope (roof and facades) conventionally concerned with insulation and sealing, to include dynamic (seasonal or daily variation) and active features (energy production and augmented ventilation). Photovoltaic (PV) systems offer local electricity generation and temperature control by natural or forced convection. The inherent heating of crystalline silicon cells can be overcome by natural (BIPV) or forced (PV-T) convection. The performance of such integrated PV systems is highly sensitive to the design, and since the demand for PV systems fully integrated into the building frames (facade, roof) is still quite recent, few studies are currently available on the subject. The Ressources project aims to advance the understanding of double-skin configurations. Three prototypes were designed: one for an existing office building facade and two for detached houses. The facade configuration was selected as it offers the largest potential surface for BIPV.

2 BIPV in double-skin structure

2.1 Structure description and operating principle

To date most double-skin components consist of a primary building facade and a secondary photovoltaic facade separated by an air gap, together comprising a solar chimney to drive natural ventilation or cool both PV and building envelope, while generating electricity throughout the year (Figure 1).

The aims of the Ressources project are first to promote PV facade cooling under critical thermal conditions (summer/natural convection) and later to consider heat recovery during winter (Figure 1(b)).

2.2 State of the art for naturally ventilated configuration

Two complementary approaches are commonly adopted to study BIPV configuration and the implied phenomena. The first concerns the global response of a system via a determination of the mass flow rate under laminar and

*This article is a part of a Special Issue on the International Conference on Energy Security, Global Warming and Sustainable Climate (SOLARIS 2012).

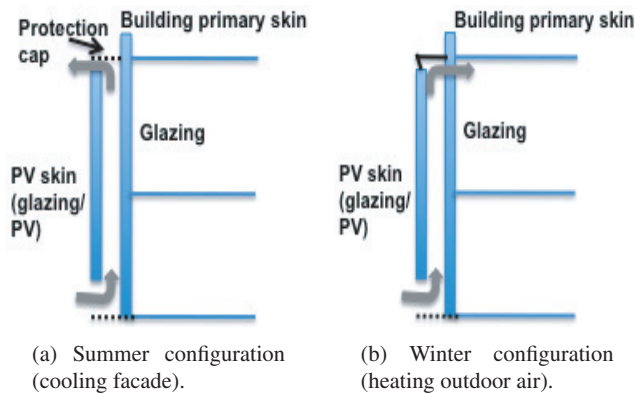


Figure 1: Operating principal of the double skin in addition to classical envelope function.

turbulent regimes [10], the complete pressure loss (including wind effects), and temperature difference between the inlet and the outlet of the channel, assuming thermal stratification in the channel [1]. Following the same global approach, numerical models can be validated using experimental measurements, and by this means the thermal and electrical performance has been evaluated [5]. In parallel, Mei et al. [8] present a dynamical model for a PV facade assembly with a single zone building model. Infield et al. [7] showed that the thermal performance of partially transparent ventilated PV facades can be described by four parameters: the heat loss from the interior to exterior, the heat loss from the interior by ventilation, and the direct transmitted and absorbed radiation gains to the interior. Other studies present experimental evaluations of full-scale systems [11,2] and characterize the thermal and kinematic behavior for specific mixed convection configurations.

The second approach relies on a full simulation and detailed experimental study as a means to identify opportunities to increase heat transfer at the fluid—PV interface—and thereby decrease the temperature of PV cells. As this general problem has many engineering applications these aspects have been tackled in a large number of studies [9,3]. This approach can also better characterize the basic phenomena that drive both the chimney effect and heat transfer [4,6].

3 Description of the prototype and experimental apparatus

Designed for a facade obliquely oriented to the south, the prototype comprises a series of adjacent prism structures constructed from metal and tinted glass, and with PV modules installed on the south-facing surfaces (Figure 2). The double facade (Figure 3) is 7.40 m high and 4 m wide, and is positioned 60 cm in front of the existing building facade to give an air gap of 60 cm to 80 cm.



Figure 2: Basic prism element of the frame.



Figure 3: Double-skin prism facade.

The thermal characteristics are measured by K-type thermocouples of 1 mm diameter located on or behind the central column of prisms. 16 thermocouples are located on each side of the double skin: 10 thermocouples attached to the PV surface in the middle of modules, and 6 on glass

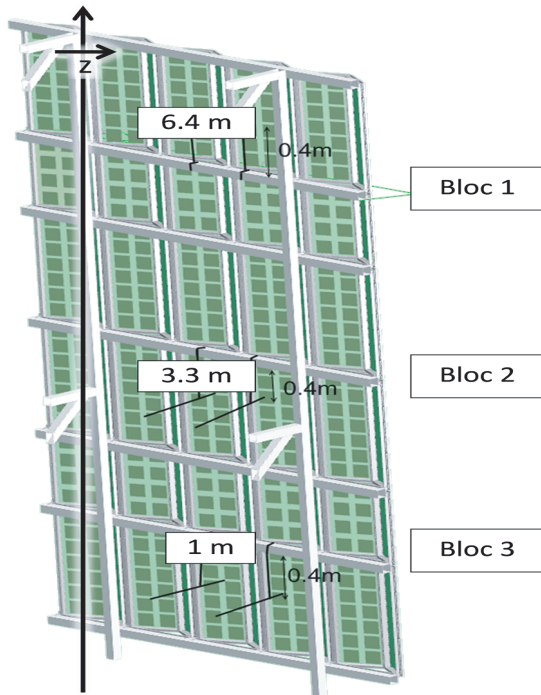


Figure 4: Spatial arrangement of “peignes” in the air gap.

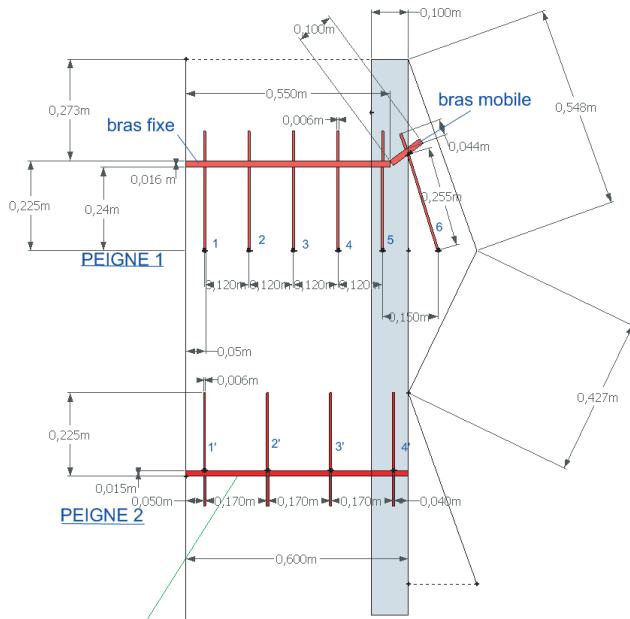


Figure 5: Thermocouples and velocity probes spatial repartition in the air gap.

surfaces (Figure 3). More 10 thermocouples are located on the primary building facade at the same vertical positions as those of the PV thermocouples. The surface is glazed and opaque, closely resembling the open section visible to the side of the prototype in Figure 3. All surface thermocouples are protected from radiation by aluminized pellets.

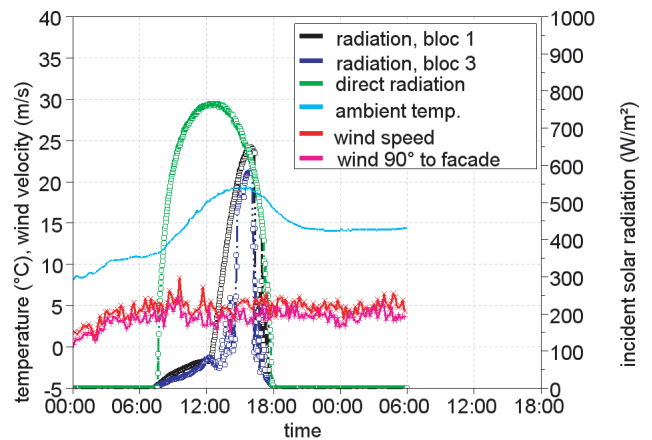
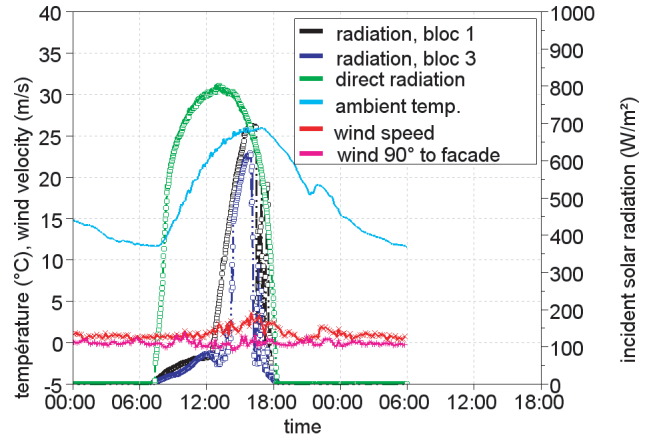


Figure 6: Radiation, temperature, and wind for one sunny day (above) and one windy day (below).

As shown in Figures 4 and 5, thin tube frame assemblies, hereafter referred to as “peignes,” were hung from the metal structure, allowing velocity and temperature probes to be added in the air gap along axes perpendicular to the facade. Vertical velocity components in both the narrower peigne “2” and wider peigne “1” could be measured within the range [0,2] m/s at three vertical locations: 1 m, 3.3 m, and 6.4 m from the bottom of the facade (Figure 4). Total horizontal incident radiation was measured by 3 pyranometers, one on the building roof and two on the upper and lower blocs of prisms (aligned with PV face) to take into account variations in albedo. A sun-tracking pyrheliometer was installed to record direct solar radiation. The spectral ranges of the pyranometers are [200,3600] nm.

4 Results

Two typical sunny days were selected in order to identify the effect of wind. As shown by Figure 6, apart from wind and ambient temperature, the days were very similar. For the windy day, a significant wind was present during the day and night, with a predominant direction of 38.4° to the normal of the facade and a mean value of 16.6 km/h. Figure 7 shows

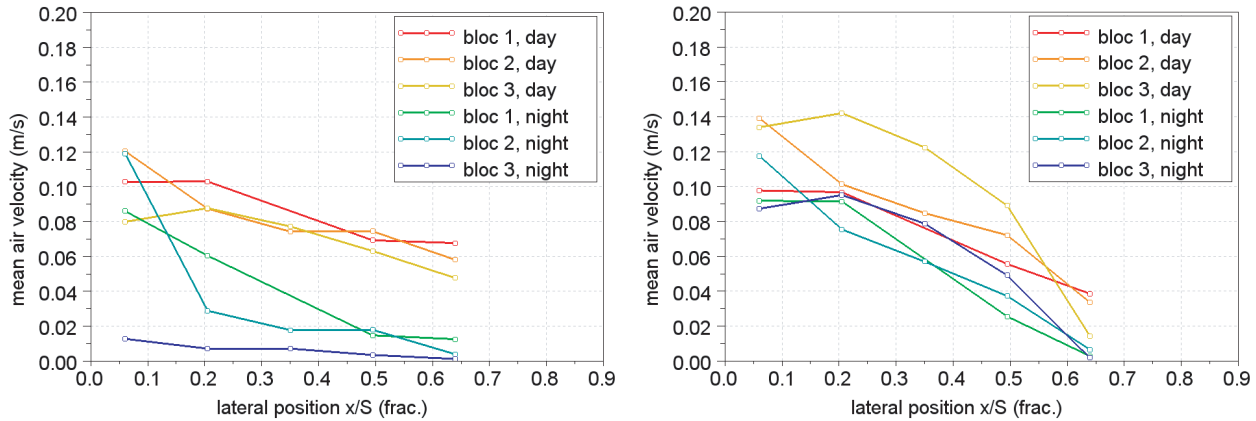


Figure 7: Mean velocity profile between the external and internal facades for a typical sunny day (left) and a typical sunny and windy day (right).

Table 1: Mean data in the air gap.

Localization	Mass flow rate (kg/s)		$[T_{\text{mean}}]T_{\text{mean}} - T_{\text{ambient}} [^{\circ}\text{C}]$	
	Sunny	Sunny & Windy	Sunny	Sunny & Windy
Bloc 1	0.117	0.099	[31.7]6.3	[25.18]6.2
Bloc 2	0.121	0.124	[29.2]3.7	[22.88]3.9
Bloc 3	0.121	0.135	[28.1]2.7	[22.06]3.0

air velocity profiles for peigne 1 between the building ($x/S = 0$) and the PV facades ($x/S = 1$ peigne 1, Figure 5) for both days. Mean daytime and nighttime wind speeds are presented for each bloc. The mean values for the days have been calculated for a period from 6 a.m. to 6 p.m., whereas for the night they are calculated from 6 p.m. to 6 a.m.

The probes situated closest to the edge of the prism were unfortunately found to be faulty. In the left graph, velocity profiles for the non-windy day show two separate trends during the day and night. In contrast, daytime and nighttime trends were similar for the windy day. When these trends are compared, it turns out that the effect of wind effect is clearly significant. Moreover, we can deduce from the lower bloc profiles that the wind is entering from the bottom of the facade. Extracted afternoon mean mass flow rates and temperatures presented in Table 1 support this observation. A constant air density (1.2 kg/m^3) has been chosen and the prism section has been selected for mass flow rate evaluation. Purely temperature-induced flow (sunny day) exhibits mean velocities that increase with height, consistent with the chimney effect. However for the windy day, the mean velocities are greatest for the lower bloc. Hence wind dominates buoyancy-induced ventilation. In this configuration a cap effect appears to be evident, and it is caused by the outlet rain protection structure. Indeed the outlet section is smaller than the inlet one. As a consequence this cap effect generates a strong 3D flow.

During the daytime, wind velocities appear slightly higher near the building facade than close to the double

facade. This may be the result of a larger pressure loss behind the PV facade due to the metal structure. Surface temperatures of the two facades do not account for this observation: at its peak, the outer PV surface was hotter than the building wall (at bloc 2) by 15.0°C and 11.8°C for the sunny and sunny-windy days, respectively (Figure 8). During the night, the lateral variation in velocity is clearly visible, with a higher velocity near the building revealing heat release to air the cavity.

Figure 8 shows the temperature evolution of each thermocouple at the level of bloc 2, including PV surface temperature (outer and inner face), air gap temperatures (peigne 1), and also the surface temperature of the building facade.

The maximum temperature differences observed in the air gap during the sunny day and the sunny-windy day were 2.9°C and 3.1°C , respectively. The largest discrepancy observed between the two days concern PV temperatures, indicating that although the wind greatly influences the temperature of PV, it is through convective exchanges on the external side of the PV facade. This lower operating temperature level has a positive impact on the electrical performance ratio, which was consistently 5–10% greater for the lower bloc of PV. The wind does not seem to affect the thermal state in the air gap to the extent observed in velocity profiles.

5 Discussions and conclusions

We have presented the first experimental observations of an innovative double-skin PV facade, with natural convection corresponding to a summer operational mode. A significant impact on building temperature is apparent from the measured temperatures of the building and PV facades. Two days were selected in order to highlight the influence of a limited number of parameters: essentially wind and external temperature. The wind effect was found to dominate and

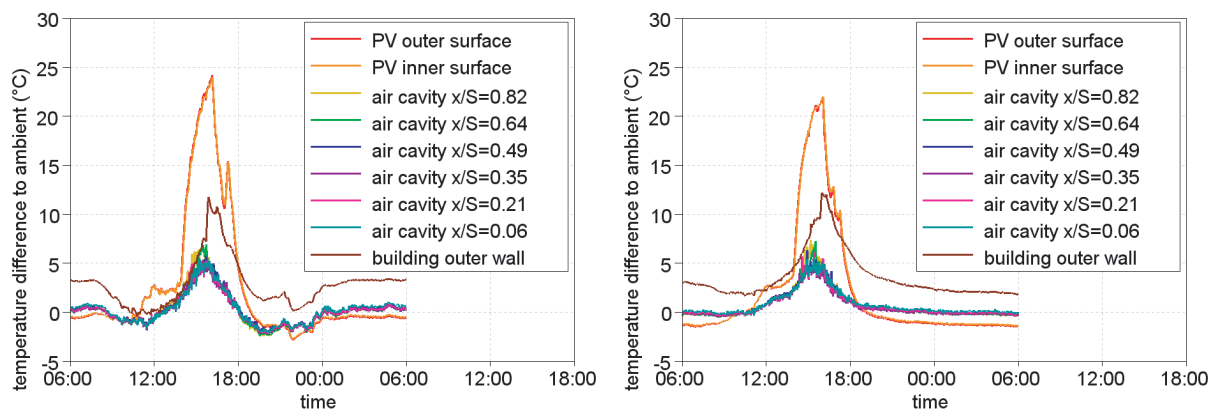


Figure 8: Mean temperature profiles relative to ambient temperature from external PV facade to building facade, for sunny (left) and sunny and windy days (right).

to contribute positively to the buoyancy effect. Air velocity trends are consistent with buoyancy-induced ventilation. The wind significantly cooled PV surfaces through external transfer, but other temperatures were not strongly affected. In contrast, the kinematic behavior of the cavity is strongly influenced by the wind. A similar approach to identify governing phenomena will be applied to data to be collected over more than one year.

Acknowledgments This work was carried out as a contribution to the French National Research Agency program PREBAT managed by the ADEME and entitled Ressources (Convention ADEME 0705C0076). The help from the partners, EDF R&D, HBS-Technal, Jacques Ferrier Architectes, LOCIE (Univ. Savoie), LEEVAM (Univ. Cergy), is acknowledged.

References

- [1] B. J. Brinkworth, *Estimation of flow and heat transfer for the design of PV cooling ducts*, *Solar Energy*, 69 (2000), 413–420.
- [2] T.-T. Chow, Q. Zhongzhu, and L. Chunying, *Potential application of “see-through” solar cells in ventilated glazing in Hong Kong*, *Solar Energy Materials and Solar Cells*, 93 (2009), 230–238.
- [3] A. G. Fedorov and R. Viskanta, *Turbulent natural convection heat transfer in an asymmetrically heated, vertical parallel-plate channel*, *International Journal of Heat and Mass Transfer*, 40 (1997), 3849–3860.
- [4] M. Fossa, C. Ménézo, and E. Leonardi, *Experimental natural convection on vertical surfaces for building integrated photovoltaic (BIPV) applications*, *Experimental Thermal and Fluid Science*, 32 (2008), 980–990.
- [5] H. P. Garg and R. S. Adhikari, *Performance evaluation of a single solar air heater with N-subcollectors connected in different combinations*, *International Journal of Energy Research*, 23 (1999), 403–414.
- [6] C. Giroux-Julien, S. Ménézo, J. Vareilles, H. Pabiou, M. Fossa, and E. Leonardi, *Natural convection in nonuniformly heated channel with application to photovoltaic facades*, *Computational Thermal Sciences*, 1 (2009), 231–258.
- [7] D. Infield, U. Eicker, V. Fux, L. Mei, and J. Schumacher, *A simplified approach to thermal performance calculation for building integrated mechanically ventilated PV facades*, *Building and Environment*, 41 (2006), 893–901.
- [8] L. Mei, D. Infield, U. Eicker, and V. Fux, *Thermal modelling of a building with an integrated ventilated PV façade*, *Energy and Buildings*, 35 (2003), 605–617.
- [9] M. Miyamoto, Y. Katoh, J. Kurima, and H. Saki, *Turbulent free convection heat transfer from vertical parallel plates*, in *Heat Transfer 1986: Proceedings of the 8th International Heat Transfer Conference*, Hemisphere, Washington, DC, 1986, 1593–1598.
- [10] M. Sandberg and B. Moshfegh, *Buoyancy-induced air flow in photovoltaic facades*, *Building and Environment*, 37 (2002), 211–218.
- [11] A. Zöllner, E. R. F. Winter, and R. Viskanta, *Experimental studies of combined heat transfer in turbulent mixed convection fluid flows in double-skin-facades*, *International Journal of Heat and Mass Transfer*, 45 (2002), 4401–4408.